

Article

Removal of Nitrate Nitrogen from Municipal Wastewater Using Autotrophic Denitrification Based on Magnetic Pyrite

Bowei Zhang ¹, Changsheng Zhao ^{1,*}, Ting Liu ² and Xiaokai Wang ¹

¹ Shandong Analysis and Test Center, College of Environmental Science and Engineering, Qilu University of Technology (Shandong Academy of Sciences), Jinan 250014, China; zbw19990110@163.com (B.Z.); wangxiaokai981025@163.com (X.W.)

² Yongrun Environmental Protection Consulting Co., Ltd., Jinan 250014, China; 17862072760@163.com

* Correspondence: zhaochsh1980@163.com; Tel.: +86-186-7881-7810

Abstract: As the problem of eutrophication of water bodies and nitrate pollution of surface and groundwater is becoming more and more prominent, deep denitrification of wastewater can effectively reduce the amount of nitrate nitrogen (NO_3^- -N) discharged into natural water bodies. To solve this problem, in this research, the autotrophic denitrifying bacteria were incorporated in an autotrophic denitrification simulator equipped with magnetic pyrite to remove NO_3^- -N and total nitrogen (TN) from wastewater. The purified strains were inoculated into municipal sewage. When the ratio of magnetic pyrite to quartz sand was 1:1 and the particle size of the filler was 0.5–1 mm, the removal rate of NO_3^- -N and TN was optimized, at 93.52% and 83.22%, respectively. Sulphate (SO_4^{2-}) concentrations will level off during stable system operation, and SO_4^{2-} concentrations show a positive correlation with NO_3^- -N and TN removal. The 16s rDNA sequencing analysis of the screened sludge showed that the main phyla in the screened and purified sludge were *Epsilonbacteraeota* and *Proteobacteria*, with an abundance of 65.83% and 26.88%, and the final enriched products were dominated by *Sulfurimonas* and *Thiobacillus*, with an abundance of 64.91% and 9.32%, respectively. The results showed that autotrophic denitrifying bacteria could be screened and purified using thiosulfate as a substrate, and that the use of magneto pyrite as an electron donor reduced most of the NO_3^- -N to N_2 , while reducing the TN content.



Citation: Zhang, B.; Zhao, C.; Liu, T.; Wang, X. Removal of Nitrate Nitrogen from Municipal Wastewater Using Autotrophic Denitrification Based on Magnetic Pyrite. *Water* **2023**, *15*, 4292. <https://doi.org/10.3390/w15244292>

Academic Editor: Stefano Papirio

Received: 24 November 2023

Revised: 13 December 2023

Accepted: 14 December 2023

Published: 16 December 2023



Copyright: © 2023 by the authors. Licensee MDPI, Basel, Switzerland. This article is an open access article distributed under the terms and conditions of the Creative Commons Attribution (CC BY) license (<https://creativecommons.org/licenses/by/4.0/>).

Keywords: nitrate pollution; municipal sewage; anaerobic sludge; autotrophic denitrification; magnetic pyrite

1. Introduction

Agricultural and industrial production has accelerated in tandem with the increase in urbanization. Due to a combination of factors, including outdated technology, resource depletion and shortages, and a general increase in environmental pollution, the poor quality of freshwater resources is of increasing concern. The discharge of large amounts of industrial wastewater and domestic sewage, containing high concentrations of nitrogen, into water bodies leads to eutrophication and destroys the ecological balance of aquatic systems. Therefore, environmental problems caused by excess total nitrogen (TN), especially nitrate nitrogen (NO_3^- -N), have received increasing attention from the government and scientists [1,2]. In a study by Leng P. et al. [3], in which surface water nitrate data in the Bohai Rim from 2001 to 2015 was analyzed, it was found that nitrate pollution was on the rise overall, and the nitrate pollution of groundwater was also increasing owing to the impact of agricultural surface sources and sewage discharge.

Conventional water treatment processes are no longer able to meet the nitrogen discharge requirements, so the development of efficient and economical nitrogen removal technologies is imperative [4]. Autotrophic denitrification in place of heterotrophic denitrification in sulfur-limestone composites has received much attention in the field of deep

nitrogen removal. Additional carbon sources are required in this system, increasing the cost of removal [5], in contrast to sulfur-limestone composites, magnetic pyrite is commonly used as a particulate medium for biofilm formation and can provide a reducing environment for denitrification [6]. In an autotrophic denitrification batch experiment with magnetite pyrite, Liu et al. [7] found that denitrification of nitrate nitrogen could be achieved by magnetite pyrite in the presence of sulfur autotrophic denitrifying bacteria. Li et al. [8] have demonstrated that NO_3^- -N reduction in sediments containing magnetic pyrite is a biological denitrification process using magnetic pyrite as an electron donor. Wei et al. [9] used autotrophic microorganisms to remove NO_3^- -N from wastewater using iron sulfide chemical sludge with iron hydroxide and ferrous sulfide as the main components as substrates.

Reduced sulfur (sulfide, sulfur monomers, thiosulfate, etc.) is a typical and cheap electron donor, and the by-products (including sulfate) produced during denitrification are less harmful than secondary pollution [10]. Currently, sulfur monomers are one of the most commonly used electron donors today, but alkalinity depletion can lead to a significant drop in pH, which inhibits the process, requiring either an external base or an increase in alkalinity in the filler to balance the pH, resulting in increased effluent hardness [11]. Due to its high water solubility, non-toxicity, and non-inhibitory properties, thiosulfate is more easily utilized in biological oxidation compared to sulfide and sulfur monomers, and is commonly used in the cultivation of sulfur autotrophic denitrifying microorganisms for their enrichment. The use of thiosulfate as an electron donor facilitates the rapid start-up of the biochemical system, which is able to minimize the production of sludge, and significantly reduces the energy consumption for sludge post-treatment and the emission of greenhouse gases [12]. Trouve et al. [13] compared the rate of NO_3^- -N reduction by *Thiobacillus* denitrificans using FeS, $\text{S}_2\text{O}_3^{2-}$, FeS_2 , and S. The autotrophic denitrification reaction rates of the four substrates decreased in the following order: $\text{S}_2\text{O}_3^{2-} > \text{FeS} > \text{FeS}_2 > \text{S}$.

On the basis of these previously published findings, we aimed to provide an efficient and low-energy-consuming method for NO_3^- -N removal through screening and purifying autotrophic denitrifying bacteria from the anaerobic sludge of a municipal wastewater treatment plant. With thiosulfate as a substrate, we inoculated the screened and purified bacterial broths, using magnetite pyrite as an electron donor. The feasibility of using this material for autotrophic denitrification was evaluated and the denitrifying capacity was measured. The results provide a reference for the removal of NO_3^- -N and the control of TN in surface waters.

2. Materials and Methods

2.1. Experimental Materials

Natural magnetic pyrite was purchased from Tongling City, Anhui Province. After crushing and screening, magnetic pyrite particles with sizes of 0.500–1.00 mm, 2.00–3.00 mm, and 5.00–10.0 mm were obtained. The particles were immersed in 10% HCl solution to remove surface oxides and then rinsed with deionized water until the pH value of the rinse solution reached neutrality. Subsequently, the particles were dried, sealed, and stored. Quartz sand was purchased from Zhuhai, Guangdong Province. The quartz was crushed and then sieved to obtain quartz sand particles sized 0.500–1.00 mm, 2.00–3.00 mm, and 5.00–10.0 mm. The particles were rinsed with deionized water, dried, and sealed for storage. The municipal sewage for the experiment was taken from a domestic sewage treatment plant in Jinan City, Shandong Province, and the anaerobic sludge was taken from the return sludge of a waste treatment plant in Jinan City, Shandong Province. The KNO_3 used in the experiments was of superior purity, and the $\text{Na}_2\text{S}_2\text{O}_3 \cdot 5\text{H}_2\text{O}$, KH_2PO_4 , NaHCO_3 , NH_4Cl , $\text{MgCl}_2 \cdot 6\text{H}_2\text{O}$, and $\text{FeSO}_4 \cdot 7\text{H}_2\text{O}$ were of analytical purity.

2.2. Denitrification Batch Experiments

Twelve batch experiments were conducted to investigate the effects of different packing ratios and packing particle sizes on the autotrophic denitrification performance of magnetic pyrite. Experiments were conducted in two stages.

To study the effect of different packing ratios on the performance of autotrophic denitrification of magnetite pyrite, 800 mL of actual wastewater was added to each device, and three different kinds of packing (T1, T2, and T3) were added, inoculated with strains after screening and purification, and then blown off with nitrogen for 10 min to maintain the anaerobic state. The temperature of the reaction mixture was maintained at 25 °C.

To study the effect of filler particle size on the autotrophic denitrification of magnetite pyrite, 800 mL of actual wastewater was added to each device, and fillers of differently sized particles (P1, P2, and P3) were added. The mixture was inoculated with strains of screened and purified bacteria and then blown off with nitrogen for 10 min to maintain the anaerobic state. The temperature of the reaction mixture was maintained at 25 °C.

2.3. Culture of Microorganisms

The dry reagents, consisting of 5 g $\text{Na}_2\text{S}_2\text{O}_3 \cdot 5\text{H}_2\text{O}$, 2 g KNO_3 , 2 g KH_2PO_4 , 1 g NaHCO_3 , 0.5 g $\text{MgCl}_2 \cdot 6\text{H}_2\text{O}$, 0.5 g NH_4Cl , and 0.01 g $\text{FeSO}_4 \cdot 7\text{H}_2\text{O}$ were weighed and added to 1000 mL of liquid medium before inoculation with 50 mL of anaerobic sludge. The conical flask was sealed with a rubber stopper containing two glass tubes, A and B. Tube A was washed with pure N_2 for 10 min to remove the air and tube B was connected to another conical flask to collect the N_2 produced. It was then sealed and incubated at 24 °C. The conical flask was then sealed and incubated at 24 °C. The success of the microbiological culture was demonstrated by the volume of gas produced (measured using the drain method, Figure 1). After four incubations, the volume of gas stabilized at approximately 240 mL per incubation, indicating successful microbial cultivation. The theoretical volume of N_2 was calculated according to the following formula, with the amount produced equal to 240.4 mL, $0.625 \text{S}_2\text{O}_3^{2-} + \text{NO}_3^- + 0.125 \text{H}_2\text{O} \rightarrow 1.25 \text{SO}_4^{2-} + 0.5 \text{N}_2 + 0.25 \text{H}^+$ [14].

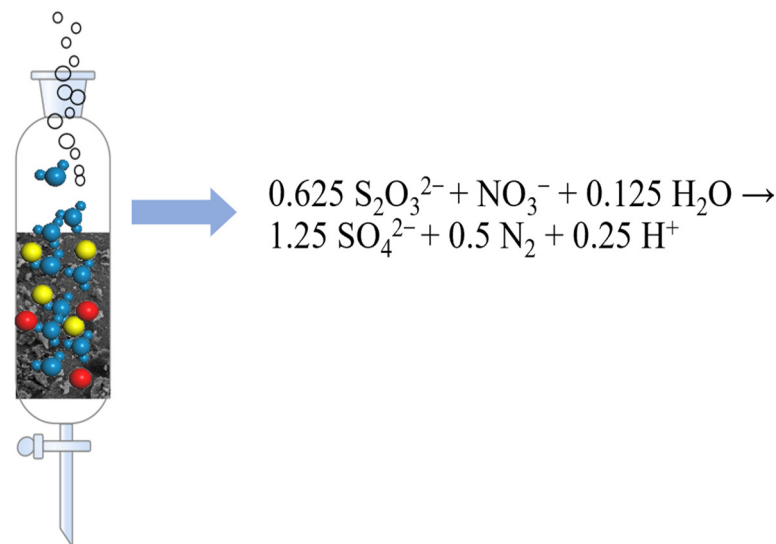


Figure 1. Diagram of the autotrophic denitrification unit.

2.4. Chemical Testing

The content of NO_3^- -N, sulfate, and TN was determined as follows. The amount of NO_3^- -N and sulfate was determined through ion chromatography (HPIC, CIC-D160, Qingdao Shenghan Chromatograph Technology Co., Ltd., Qingdao, China) [15], and TN was measured by using alkaline potassium persulfate digestion UV spectrophotometry (Ultraviolet visible spectrophotometer, 759S, Shanghai Spectrum Analyzer Co., Ltd., Shanghai, China) [16]. Incubated inoculums were stored at -80 °C for subsequent experiments.

The two specimens were centrifuged, washed, and centrifuged again, repeating the operation 3–4 times. The supernatant was discarded, and the precipitated DNA was extracted with a soil DNA kit, the detailed procedure of which was carried out according to its instructions. DNA concentration and purity were determined using a Nanodrop 2000 spectrophotometer and detected using 1% agarose gel electrophoresis. PCR amplification was performed on the DNA genome after extraction, and the amplified fragment region was the 16s rDNA V3-V4 region, and the primers were universal primers within this region: 338F (5'-ACTCCTACGGGAGGCAGCA-3') and 806R (5'-GGACTACHVGGGTWTCTAAT-3'). The amplification process included 95 °C pre-denaturation for 3 min; denaturation at 95 °C for 30 s; annealing at 55 °C for 30 s; and extension at 72 °C for 45 s. The reaction was cycled 27 times, and the reaction was extended at 72 °C for 5 min at 12 °C until the reaction was terminated. After the PCR amplification, the results were sequenced by using Illumina NovaSeq6000 (CapitalBio Technology Co., Ltd., Beijing, China) high-throughput sequencing.

2.5. Characterization of Magnetic Pyrite

A small amount of dried sample was taken and analyzed using a Scanning Electron Microscope (SEM) and its accompanying X-ray Energy Dispersive Spectrometer (EDS).

2.6. Data Analysis

Three replicate experiments were conducted for all experiments and data are shown as mean with standard deviation. A one-way analysis of variance (ANOVA) with a 95% confidence interval was performed using SPSS19.0 statistical analysis software to analyze the significant differences between the control and the different treatments. Statistically significant differences compared to the control group are indicated by * ($p < 0.05$) and ** ($p < 0.01$) in the graphs.

3. Results

3.1. Characterization of Magnetic Pyrite

To analyze the chemical composition of the magnetic pyrite, a scanning electron microscope (SEM) and an energy-dispersive X-ray spectrometer (EDS) were used to characterize the material morphologically and analyze the elements (Table 1, Figure 2). As shown in the micrographs (Figure 2a,b), the surface of the magnetite pyrite was relatively smooth and granular with large particles. Magnetite pyrite mainly consists of S, C, O, and Fe, of which elemental sulfur has the highest percentage, accounting for 62.19% of the total, followed by Fe, O, and C, which accounted for 15.95%, 15.10%, and 5.23%, respectively. The presence of elemental O may be due to the oxidation of SO_4^{2-} by O_2 and water on the surface of the sulfurous iron ore during the washing and drying processes.

Table 1. EDS energy spectrum analysis of magnetic pyrite (%).

Element	C (%)	O (%)	S (%)	Ca (%)	Fe (%)
Percentage of atoms	5.23	15.10	62.19	1.53	15.95

3.2. Screening of Purified Strains for Autotrophic Denitrification Capacity

As can be seen in Figure 3, in the control group inoculated with seed sludge, both NO_3^- -N and TN decreased to a certain extent during the first 36 h. After 36 h, the concentrations of NO_3^- -N and TN tended to increase and then decrease, which may be because the number of autotrophic denitrifying bacteria in the seed sludge was very small and these bacteria were gradually replaced by the dominant species, ultimately leading to NO_3^- -N elevation in the system. From 0 to 144 h, the three different packing ratios, the concentration of nitrate nitrogen, and TN concentration exhibited a gradually decreasing trend, among which, T1 had the best effect, resulting in the most significant difference ($p < 0.01$), wherein the concentration of NO_3^- -N was reduced from 41.18 to 2.67 mg/L, with a removal rate of 93.52%, and the concentration of TN was reduced from 48.18 to 8.08 mg/L,

with a removal rate of 83.22%. The changes in NO_3^- -N and TN concentrations were relatively slow during the first 36 h, probably because they were in the microbial growth and acclimatization phase, after which the NO_3^- -N and TN concentrations changed at an accelerated rate (beginning at 36 h, $p < 0.01$). In a study by Torrentó et al. [17], in which simulated groundwater was passed through sulfurous pyrite reaction columns inoculated with *T. denitrificans*, the NO_3^- -N (35 mg/L) in the effluent was not completely degraded after 200 days. In another study, in which pyrite and sulfur were used as electron donors, the TN removal rate was only 19.2% after 65 d of operation of the denitrification system (Li et al.). Compared with the materials used in the above studies, magnetic pyrite as an electron donor was more efficient in removing NO_3^- -N and TN.

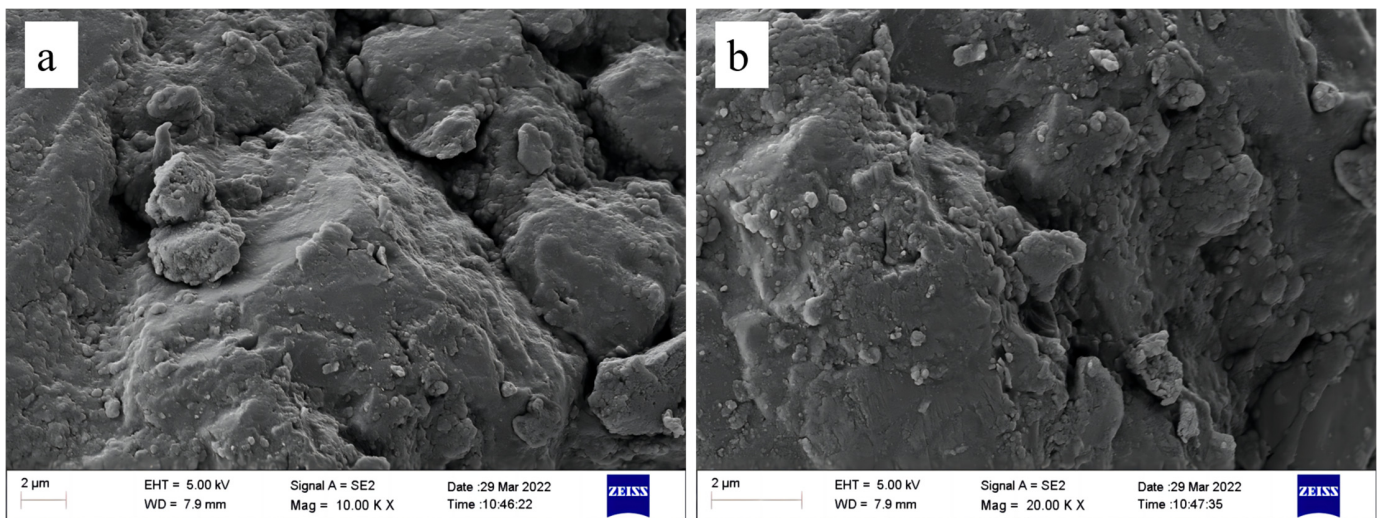


Figure 2. Characterization of magneto pyrite; (a,b) scanning electron microscopy images of magneto pyrite.

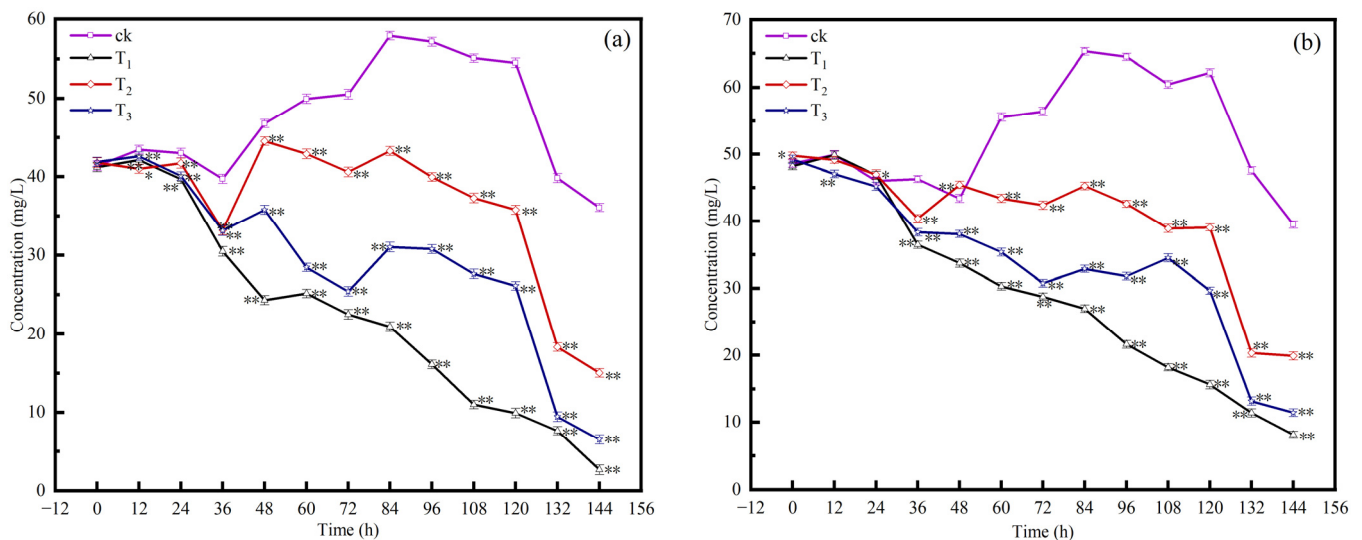


Figure 3. Effect of packing on removal rates of NO_3^- -N (a) and TN (b). T1: filler: magnetic pyrite: quartz sand = 1:1; T2: quartz sand; T3: magnetic pyrite. Statistically significant differences compared to the control group are indicated by * ($p < 0.05$) and ** ($p < 0.01$) in the graphs.

In the present study, the N removal rate of the blank group (without packing) showed a decreasing and then increasing trend (Figure 4), probably because of the presence of substances providing electron donors in the municipal wastewater in the early stage, and the concentration of NO_3^- -N increased with the depletion of electron donors in the later stage [8]. In the experimental group, with the increase in the particle size of the filler

increases, the reduction in NO_3^- -N gradually increased, with a corresponding increase in the N removal rate. In the first 24h, due to the internal system and denitrification related bacteria are difficult to adapt, microorganisms are in the growth period, denitrification is weakened, the removal rate is relatively low. After 24 h, the relevant role of the flora gradually adapted to the internal environment, and the removal rate gradually increased. When the packing particle size was 0.5–1 mm, the removal effect of NO_3^- -N and TN was optimized ($p < 0.01$), and after 144 h of autotrophic denitrification process, NO_3^- -N and TN were reduced from 41.18 and 48.18 mg/L to 2.67 and 8.08 mg/L, respectively, and the removal rate was 93.52% and 83.22%, respectively. When the filler particle sizes were 2–3 mm and 5–10 mm, after 144 h of autotrophic denitrification, the removal rate of NO_3^- -N was 65.77% and 60.80%, respectively, and that of TN was 59.24% and 55.35%, respectively. With the increase in packing particle size, the removal rate of both NO_3^- -N and TN showed a decreasing trend, and the smaller the particle size, the more readily it is utilized by autotrophic denitrifying bacteria, and consequently, the more advantageous it is for the removal of NO_3^- -N and TN.

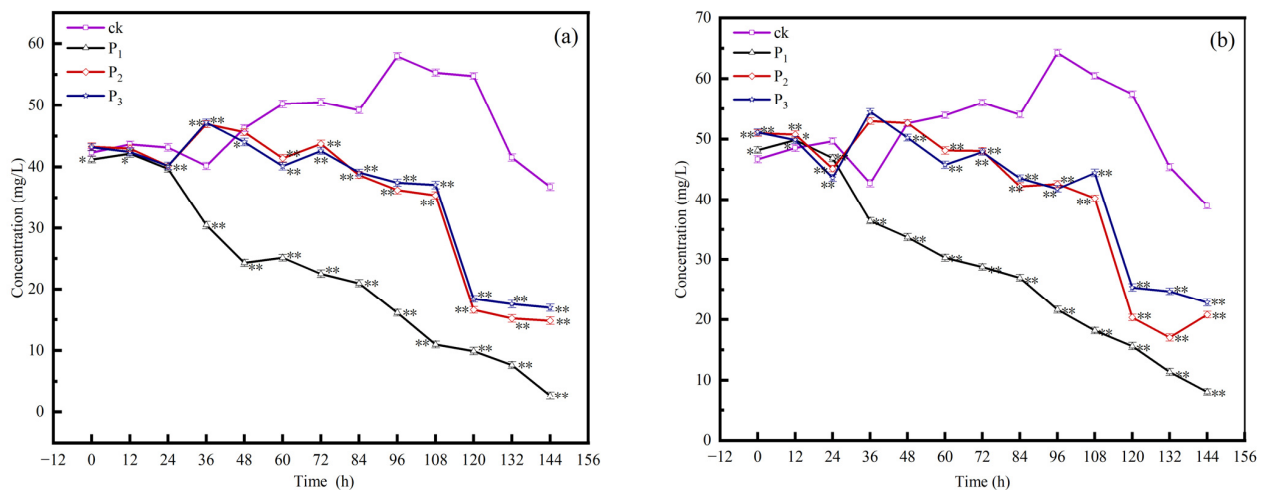


Figure 4. Effect of filler particle size on NO_3^- -N (a) and TN (b) removal rate. P1 particle size: 0.5–1 mm; P2: 2–3 mm; P3: 5–10 mm. Statistically significant differences compared to the control group are indicated by * ($p < 0.05$) and ** ($p < 0.01$) in the graphs.

The above data shows that it is feasible to screen purified denitrifying bacteria autotrophically with thiosulphate, which can reduce 93.52% of NO_3^- -N to N_2 using magnet pyrite as an electron donor. Zhang et al. [18] showed that at a relatively high initial concentration of NO_3^- -N, the removal rate was only 53% after 144h of reaction. Zhou et al. [19] used sodium thiosulphate combined with pyrite as a filler in a reactor for nitrogen removal, which maintained a maximum removal rate of more than 72%. In the present study, we achieved a higher removal rate in a shorter period.

3.3. Accumulation of Sulfate

With magnetic pyrite as the electron donor for autotrophic denitrification, the autotrophic denitrification process is hindered by sulfate production. As shown in Figure 5a, the concentration of SO_4^{2-} varied during the autotrophic denitrification process with different fillers. At the beginning of the reaction, owing to the SO_4^{2-} in the actual wastewater and original sludge medium, each system contained a small amount of SO_4^{2-} after inoculation, and the initial SO_4^{2-} concentrations of the four systems were 155, 152, 170, and 157 mg/L, respectively. In the control group, because the seed sludge was not screened and purified, the content of autotrophic denitrifying bacteria was low, and the removal rate of NO_3^- -N was low. During autotrophic denitrification, the concentration of sulfate remained essentially constant. In the experimental group, during autotrophic denitrification, the early stages of the reaction, when the autotrophic denitrifying bacteria were

in the acclimatization period, the rate of autotrophic denitrification was slower, and the increase in sulfate was also slower. In the later stage, the rate of autotrophic denitrification accelerated, the rate of sulfate production accelerated, the reaction gradually tended to complete, and the concentration of sulfate gradually remained stable for approximately 120 h. The entire process accumulated 138, 231, 273, and 225 mg/L, respectively, and the concentration of sulfate was positively correlated with NO_3^- -N and TN removal rates.

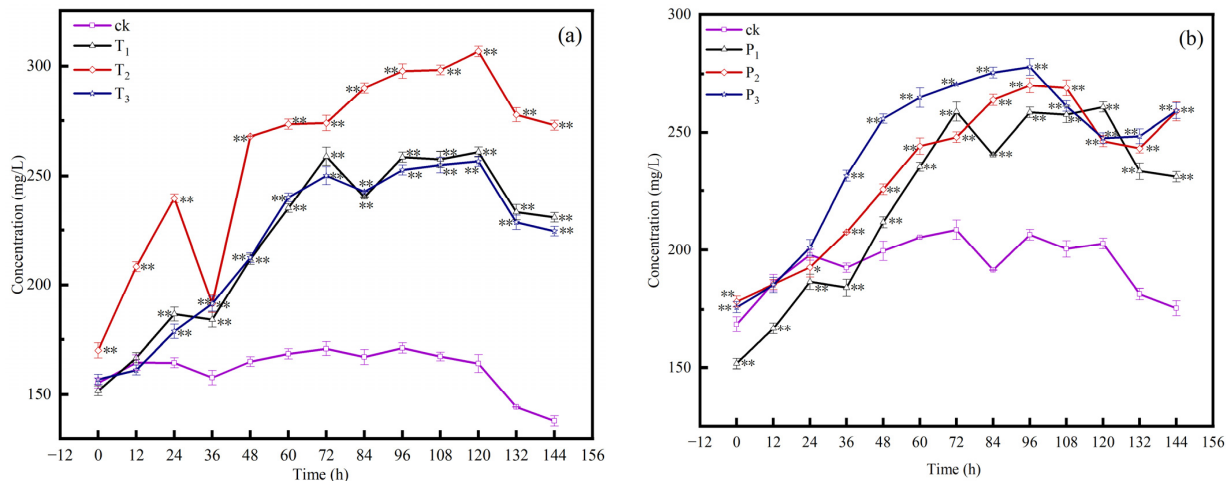
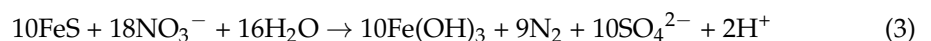


Figure 5. Effect of fillers on sulphate accumulation in wastewater (a); Effect of particle size on sulphate accumulation in wastewater (b). Accumulation of sulfate during autotrophic denitrification. T1: filler: magnetic pyrite: quartz sand = 1:1; T2: quartz sand; T3: magnetic pyrite. P1 particle size: 0.5–1 mm; P2: 2–3 mm; P3: 5–10 mm. Statistically significant differences compared to the control group are indicated by * ($p < 0.05$) and ** ($p < 0.01$) in the graphs.

As shown in Figure 5b, the concentration of sulfate first gradually increased and finally leveled off. In the early stage, the concentration of SO_4^{2-} rose rapidly due to the fact that magnetic pyrite can be oxidized by oxygen to produce SO_4^{2-} . Oxygen is mixed into the system and the substrate begins to combine with the oxygen and react to form oxides. In addition, filler added to the system may react with oxygen. At the same time, the autotrophic denitrification reaction in the system begins to consume NO_3^- -N and produce SO_4^{2-} , resulting in an initial high concentration of sulfate in the effluent, which gradually decreases and eventually stabilizes as the operation progresses. The magnetic pyrite autotrophic denitrification reaction equation and total reaction equation are as follows [14]:



In the system, the removal of NO_3^- -N and the generation of SO_4^{2-} are the key factors for the smooth running of the autotrophic denitrification process (Equation (3)). The reaction gradually accelerated with the gradual accumulation of SO_4^{2-} until the reaction was completed in approximately 120 h (Figure 5b), after which the sulfate concentration remained stable.

3.4. Analysis of Microbial Community Structure

The autotrophic denitrifying bacteria were screened using thiosulfate as the substrate, the community structure of the screened and purified sludge was analyzed by sequencing, and the samples were extracted from the screened sludge for microbial community structure analysis. The sequence composition, OTU number, and microbial community diversity of the samples were analyzed, as shown in Table 2. Approximately 68,374–71,866 valid

sequences were obtained, which corresponded to the number of samples clustered to 1235–1410. The original sequences contained optimized sequences with two-primer sequences and were then sheared and filtered using Cutadapt version 1.18 [20].

Table 2. Analysis of the sequence composition of the samples.

Number	Number of Sequences	Number of OTUs
TE-1	71,866	1410
TE-2	68,374	1235

The screened sludge samples were sequenced and analyzed, the colony structure of the samples at different taxonomic levels was observed, histograms were drawn, the species composition and abundance of the different samples were shown in histograms, and taxonomic analyses were performed on the two samples at the phylum and genus levels [21].

In Figure 6, we present the bacterial community composition of the screened sludge. The dominant phylum was *Epsilonbacteraeota*, with an average abundance of 65.83%, followed by *Proteobacteria*, *Bacteroidetes*, and *Acidobacteria*, with average abundances of 26.88%, 3.40%, and 0.86%, respectively. The four dominant taxa of bacteria accounted for 96.97% of the total community. *Epsilonbacteraeota* was initially discovered as a pathogenic bacterium, and then gradually discovered in some extreme environments with the development of gene sequencing technology. Most of the *Epsilonbacteraeota* phylum are inorganic chemo energetic autotrophic microbial populations that are capable of redox metabolism of NO_3^- and NO_2^- using reduced state sulfur [22]. The results of the study by Men et al. [23] showed that the dominant phylum was *Proteobacteria* and *Planctomycetes*, all of which were able to maintain high relative abundance. In the study by Wen et al. [18], *Betaproteobacteria* and *Epsilonproteobacteria* were the dominant phyla in the system, corresponding to relative abundances of 49.35% and 13.66%, respectively. Experiments by Ma et al. [24] showed that *Proteobacteria* (42.24–51.49%), *Chloroflexi* (17.37–23.01%), and *Planctomycetes* (19.26–22.88%) were the top three clades in the running system. In comparison, among the strains screened in the present study, *Epsilonbacteraeota* had the highest abundance (65.83%) followed by *Proteobacteria* (26.88%).

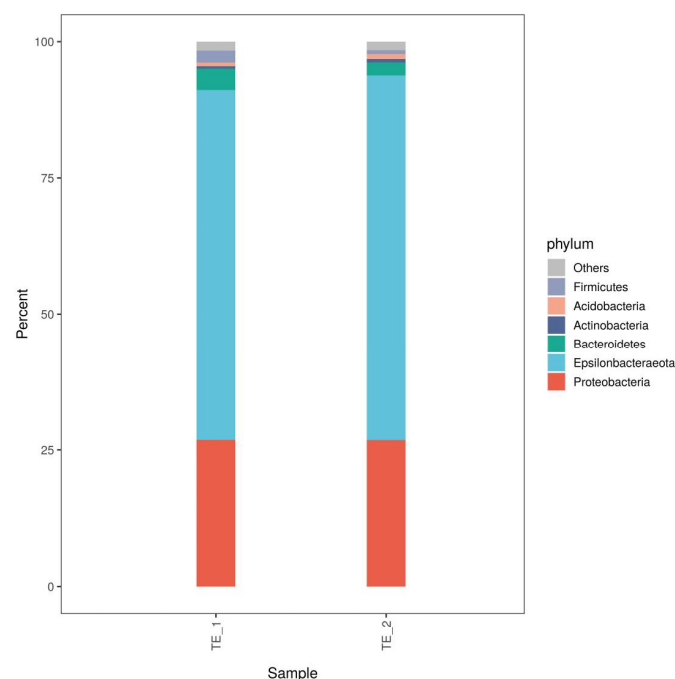


Figure 6. Community structure of samples at the gate level.

Sulfurimonas was the dominant bacteria group in the screened inoculated sludge with an average abundance of 64.91%, followed by *Thiobacillus*, *Halothiobacillus*, and *Thiomonas*, with proportions of 9.32%, 4.39%, and 2.07%, respectively, and the proportion of the four in the total community was 80.69% (Figure 7). The dominant bacterial community in the screened sludge was *Sulfurimonas*, whereas in the study by Fan et al. [25], there were only fewer *Sulfurimonas*. The dominant bacterial strain cultured by Fu et al. [26] was *Thiomonas* (51.25%), and *Sulfurimonas* accounted for a small proportion. *Sulfurimonas* and *Thiobacillus* are the most utilized sulfur-oxidizing bacteria for NO_3^- -N reduction and are typical sulfur-oxidizing nitrate-reducing bacteria, reducing NO_3^- -N while oxidizing sulfur or sulfide. The addition of these two bacteria improved the community structure in the reaction system, which in turn enhanced the nitrogen removal efficiency. Here, we successfully screened out the higher abundance of *Sulfurimonas* and a much higher proportion of both genera compared to the results of previous studies.

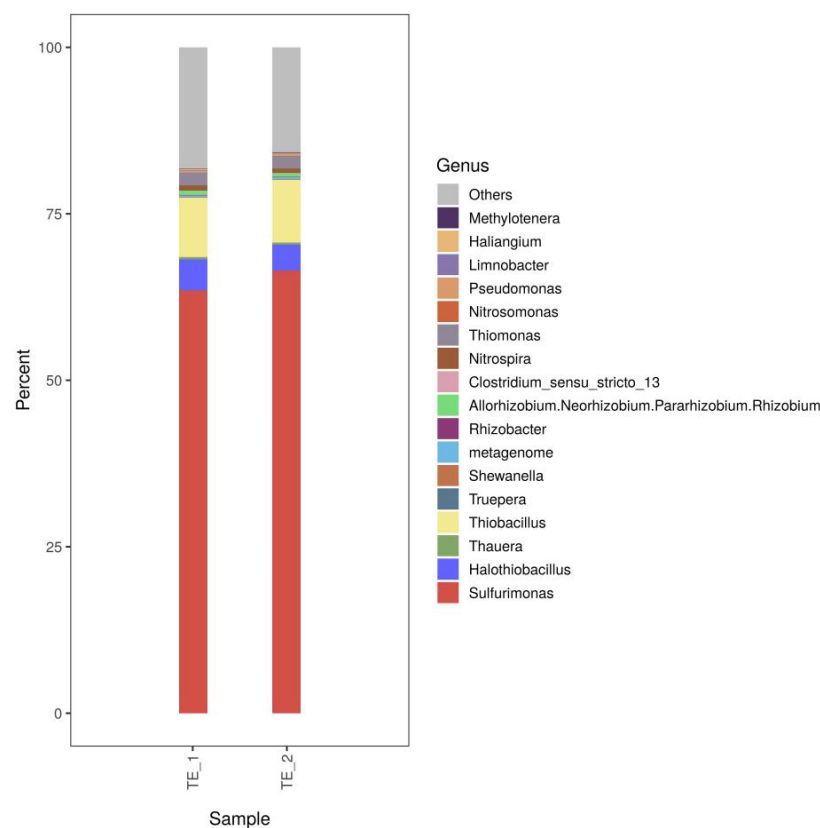


Figure 7. Community structure of samples at genus level.

As shown in Figure 8, the highest abundance of *Sulfurimonas* and *Thiobacillus* genera was found in the screened sludge. *Thiobacillus* is a dominant genus of bacteria with an autotrophic denitrification function discovered earlier, and it is easy to be enriched under the role of iron-mediated action, so as to make the nitrogen removal efficacy even better [27–29]. Studies have shown that *Thiobacillus* is capable of autotrophic denitrification of Fe (II) besides sulfur [30]. *Halothiobacillus* is a genus of gram-negative bacteria that is a strictly *chemoattractive* group of organisms. *Halothiobacillus* generally occurs singly or in pairs and is capable of oxidizing inorganic sulfur compounds in the reduced state to obtain energy, in addition to being a halophilic microorganism [31,32]. *Thiomonas* is capable of heterotrophic, autotrophic, and mixotrophic growth, and it is capable of autotrophic growth in the pH range of 2.3–9 [33].

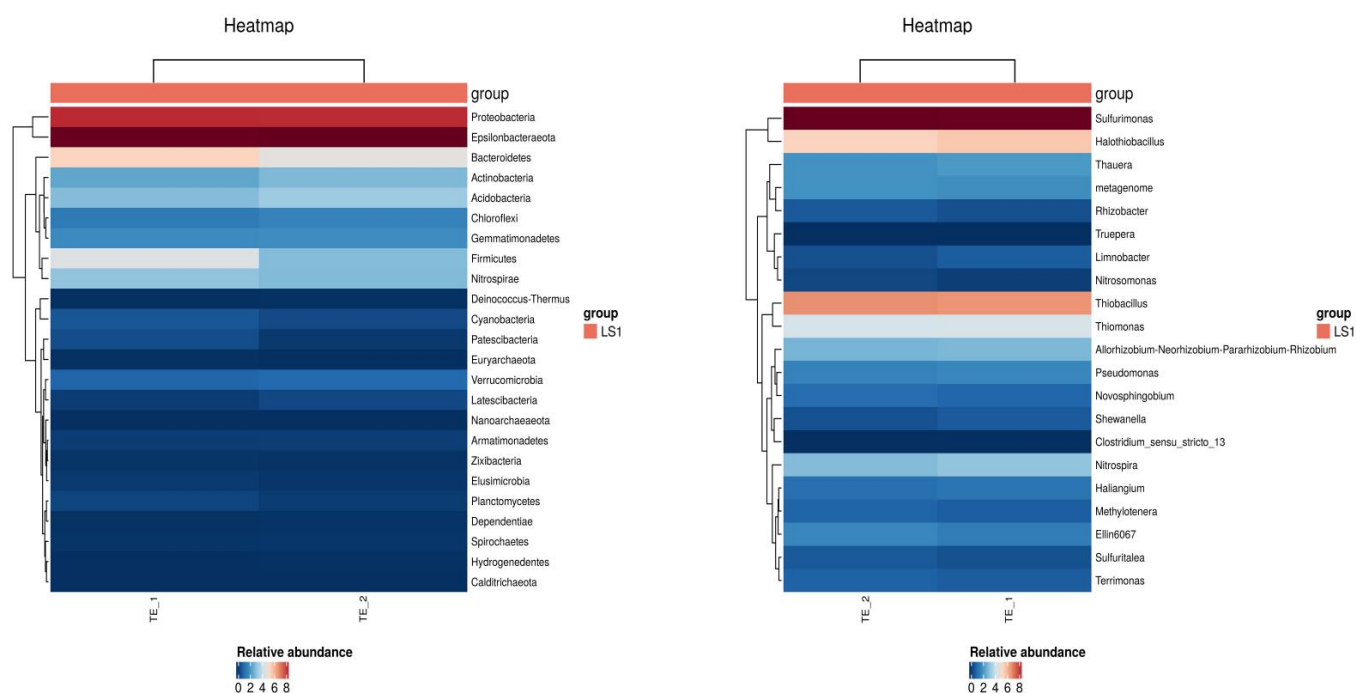


Figure 8. Thermal map of relative abundance of samples at phyla and genus levels.

4. Discussion

In this study, the screening and purification of autotrophic denitrifying bacteria was accomplished in an enriched culture setup for autotrophic denitrifying bacteria using thiosulfate as a substrate and then inoculated into actual wastewater with magneto pyrite as an electron donor in a small pilot experiment. The autotrophic denitrification of magneto pyrite provides a referable theoretical basis for the removal of NO_3^- -N from wastewater and the control of TN in water bodies, which is of great significance to alleviate the eutrophication problem prevailing in water bodies at present.

Natural magnetite pyrite is a sulfide mineral with large reserves in nature, and it is widely sourced and has a low production cost, combining microbial technology with magnetite pyrite can effectively improve water quality and greatly increase purification efficiency [34]. Magneto pyrite acted as an electron donor in the redox reaction, and NO_3^- -N and TN concentration decreased significantly after a certain period of time, indicating that this study was able to complete the degradation of nitrogen. In a previous study, Han et al. added magnetic pyrite carriers to a biofilter, which simultaneously increased the removal of NO_3^- -N and TN, reduced the production of SO_4^{2-} , and promoted the growth of associated functional bacteria, while reducing the investment cost by about 26% [35]. In addition, the effectiveness of the removal of nitrogen was also confirmed in the experiments of magneto pyrite biofilter by Zhang et al. The microbial community structure was changed, and the dominant bacteria of the system were *Thiobacillus* and *Sulfurimonas*, which is in agreement with our findings [36].

Previous studies have focused on the application of sulfur autotrophic denitrification in water treatment, but it requires the addition of sodium carbonate or other substances to neutralize the acid produced by the reaction. On the other hand, magnetic pyrite does not change the pH of the aqueous environment, but the internal pH of the system is stable enough to ensure nitrogen reduction [37].

At present, the research on magneto pyrite autotrophic denitrification is emerging [38–40], as a new autotrophic biological denitrification process can effectively achieve the denitrification of synthetic wastewater, surface water, municipal sewage and other denitrification treatments, but due to the high concentration of the influent water, the bioaugmentation time for autotrophic denitrifying bacteria, resulting in a relatively long hydraulic retention time, slower denitrification and the production of a certain amount of SO_4^{2-} and other prob-

lems, this method itself still needs to be further improved. Therefore, in future research, we should focus on the profound relationship between microorganisms and reactor operation and regulation conditions, and explore the combined use with other related reactors.

5. Conclusions

Epsilonbacteraeota (65.83%) and *Proteobacteria* (26.88%) as the major phylum in sieve-purified sludge, and the final enriched products were the genera *Sulfurimonas* and *Thiobacillus*, with abundances of 64.91% and 9.32%, respectively. After screening and purification, the strains were inoculated into the actual wastewater, From 0h to 144h, with three different packing ratios, the concentration of NO_3^- -N and TN have a tendency to decrease gradually, with the increase in packing particle size, the removal rate of NO_3^- -N and TN show a tendency to decrease, and the smaller the particle size, the more favorable to its removal, and when the ratio of magnetic pyrite: quartz sand was 1:1 and the particle size of the filler was 0.5–1 mm, the best removal effect of NO_3^- -N and TN was achieved, while the removal rate was 93.52% and 83.22%, respectively. As the rate of autotrophic denitrification accelerated, the concentration of SO_4^{2-} produced gradually increased, but when the reaction gradually became complete, the concentration of SO_4^{2-} gradually remained stable, and the concentration of SO_4^{2-} showed a positive correlation with the removal rates of NO_3^- -N and TN.

Author Contributions: Conceptualization, T.L.; methodology, B.Z. and T.L.; software, B.Z.; validation, B.Z.; formal analysis, B.Z.; investigation, B.Z., T.L. and X.W.; resources, T.L. and B.Z.; data curation, B.Z. and T.L.; writing—original draft preparation, B.Z. and T.L.; writing—review and editing, B.Z.; visualization, B.Z.; supervision, C.Z.; project administration, B.Z., C.Z. and T.L.; funding acquisition, C.Z. All authors have read and agreed to the published version of the manuscript.

Funding: This research was funded by the National Natural Science Foundation of China (41877041), and the Natural Science Foundation of Shandong Province (ZR2022MC204).

Data Availability Statement: Data is contained within the article.

Conflicts of Interest: Author Ting Liu was employed by the company Yongrun Environmental Protection Consulting Co., Ltd. The remaining authors declare that the research was conducted in the absence of any commercial or financial relationships that could be construed as a potential conflict of interest.

References

1. Romanelli, A.; Soto, D.X.; Matiatos, I.; Martínez, D.E.; Esquius, S. A biological and nitrate isotopic assessment framework to understand eutrophication in aquatic ecosystems. *Sci. Total Environ.* **2020**, *715*, 136909. [[CrossRef](#)] [[PubMed](#)]
2. Guo, L.; Chen, Q.; Fang, F.; Hu, Z.; Wu, J.; Miao, A.; Xiao, L.; Chen, X.; Yang, L. Application potential of a newly isolated indigenous aerobic denitrifier for nitrate and ammonium removal of eutrophic lake water. *Bioresour. Technol.* **2013**, *142*, 45–51. [[CrossRef](#)] [[PubMed](#)]
3. Leng, P.; Li, F.; Gu, C.; Zhu, N.; Qiao, Y.; Hao, S.; Du, K. Analysis of nitrate pollution in rivers around Bohai Sea Based on integrated analysis. *J. Environ. Sci.* **2018**, *38*, 1537–1548.
4. Li, H.; Li, Y.; Guo, J.; Song, Y.; Hou, Y.; Lu, C.; Han, Y.; Shen, X.; Liu, B. Effect of calcinated pyrite on simultaneous ammonia, nitrate and phosphorus removal in the BAF system and the Fe^{2+} regulatory mechanisms: Electron transfer and biofilm properties. *Environ. Res.* **2021**, *194*, 110708. [[CrossRef](#)] [[PubMed](#)]
5. Wang, L.; Liu, J.; Li, Y.; Liu, Z.; Zhang, L.; Che, H.; Cui, H.; Zhang, Y. Elemental sulfur-driven autotrophic denitrification process for effective removal of nitrate in mariculture wastewater: Performance, kinetics and microbial community. *Chemosphere* **2023**, *337*, 139354. [[CrossRef](#)]
6. Wang, M.; Qiu, X.; Yuan, Q.; Qiu, T.; Xu, R.; Yan, H. Research Status of Iron Sulfide Minerals in Wastewater Treatment. *Nonferrous Met. Sci. Eng.* **2020**, *11*, 78–84.
7. Liu, Z. *Preliminary Study on The Simultaneous Removal of Nitrate and Arsenic from Water with Nature Pyrrhotite*; Nanjing University: Nanjing, China, 2016.
8. Li, R.; Morrison, L.; Collins, G.; Li, A.; Zhan, X. Simultaneous nitrate and phosphate removal from wastewater lacking organic matter through microbial oxidation of pyrrhotite coupled to nitrate reduction. *Water Res.* **2016**, *96*, 32–41. [[CrossRef](#)]
9. Wei, Y.; Dai, J.; Mackey, H.R.; Chen, G.H. The feasibility study of autotrophic denitrification with iron sludge produced for sulfide control. *Water Res.* **2017**, *122*, 226–233. [[CrossRef](#)]

10. Wu, H.; Li, A.; Gao, S.; Xing, Z.; Zhao, P. The performance, mechanism and greenhouse gas emission potential of nitrogen removal technology for low carbon source wastewater. *Sci. Total Environ.* **2023**, *903*, 166491. [[CrossRef](#)]
11. Di Capua, F.; Pirozzi, F.; Lens, P.N.; Esposito, G. Electron donors for autotrophic denitrification. *Chem. Eng. J.* **2019**, *362*, 922–937. [[CrossRef](#)]
12. Rahimi, S.; Modin, O.; Mijakovic, I. Technologies for biological removal and recovery of nitrogen from wastewater. *Biotechnol. Adv.* **2020**, *43*, 107570. [[CrossRef](#)] [[PubMed](#)]
13. Trouve, C.; Chazal, P.M.; Gueroux, B.; Sauvaitre, N. Denitrification by new strains of *Thiobacillus denitrificans* under non-standard physicochemical conditions. Effect of temperature, pH, and sulphur source. *Environ. Technol.* **1998**, *19*, 601–610. [[CrossRef](#)]
14. Pu, J.; Feng, C.; Liu, Y.; Li, R.; Kong, Z.; Chen, N.; Tong, S.; Hao, C.; Liu, Y. Pyrite-based autotrophic denitrification for remediation of nitrate contaminated groundwater. *Bioresour. Technol.* **2014**, *173*, 117–123. [[CrossRef](#)] [[PubMed](#)]
15. Ministry of Environmental Protection. *Water Quality-Determination of Inorganic Anions (F^- , Cl^- , NO_2^- , Br^- , NO_3^- , PO_4^{3-} , SO_3^{2-} , SO_4^{2-})-Ion Chromatography*; HJ 84-2016; China Environmental Science Press: Beijing, China, 2016.
16. Ministry of Environmental Protection. *Water Quality-Determination of Total Nitrogen-Alkaline Potassium Persulfate Digestion UV Spectrophotometric Method*; HJ 636-2012; China Environmental Science Press: Beijing, China, 2012.
17. Torrentó, C.; Cama, J.; Urmeneta, J.; Otero, N.; Soler, A. Denitrification of groundwater with pyrite and *Thiobacillus denitrificans*. *Chem. Geol.* **2010**, *278*, 80–91. [[CrossRef](#)]
18. Zhang, W. *Simultaneous Removal of Nitrogen and Phosphorus from Secondary Effluent by Autotrophic Denitrification Based on Pyrite*; China University of Geosciences: Beijing, China, 2019.
19. Zhou, Y.; Mai, W.; Dai, J.; Sun, P.; Zeng, L.; Tang, Q. Study on autotrophic denitrification performance of sodium thiosulfate combined with pyrite system. *China Environ. Sci.* **2020**, *40*, 2081–2086.
20. Martin, M. Cutadapt removes adapter sequences from high-throughput sequencing reads. *EMBnet. J.* **2011**, *17*, 10–12. [[CrossRef](#)]
21. Oberauner, L.; Zachow, C.; Lackner, S.; Högenauer, C.; Smolle, K.H.; Berg, G. The ignored diversity: Complex bacterial communities in intensive care units revealed by 16S pyrosequencing. *Sci. Rep.* **2013**, *3*, 1413. [[CrossRef](#)]
22. Cheng, M.; Chen, Z.; Wang, A.; Zhang, S.; Li, N.; Liang, Z.; Lai, J.; Kang, P.; Liang, Y.; Yu, G. Remediate black-odorous sediment by slow-release calcium nitrate: Migration, transformation and microbial succession. *J. Clean. Prod.* **2023**, *413*, 137458. [[CrossRef](#)]
23. Men, Y.; Liu, L.; Zhu, Y.; Bi, Y.; Meng, F.; Yu, J.; Wang, S. Effect of Organic Matter Concentration Variation on Nitrogen Removal Performance and Bacteria Community Structure in a Hybrid SBR Anammox System. *Environ. Eng.* **2023**, *41*, 83–90.
24. Ma, J.; Wei, J.; Kong, Q.; Li, Z.; Pan, J.; Chen, B.; Qiu, G.; Wu, H.; Zhu, S.; Wei, C. Synergy between autotrophic denitrification and Anammox driven by FeS in a fluidized bed bioreactor for advanced nitrogen removal. *Chemosphere* **2021**, *280*, 130726. [[CrossRef](#)]
25. Fan, C.; Zhou, W.; He, S.; Huang, J. Sulfur transformation in sulfur autotrophic denitrification using thiosulfate as electron donor. *Environ. Pollut.* **2021**, *268*, 115708. [[CrossRef](#)] [[PubMed](#)]
26. Fu, B.; Pan, J.; Ma, J.; Wang, F.; Wu, H.; Wu, C. Deep removal of total nitrogen from coking wastewater using sulfur-containing iron chemical sludge as denitrification electron donor. *Environ. Sci.* **2018**, *39*, 3262–3270.
27. Zhou, L.; Lai, Y.; Shao, Z.; Jian, Y.; Zhuang, W.Q. Keystone bacteria in a thiosulfate-driven autotrophic denitrification microbial community. *Chem. Eng. J.* **2023**, *470*, 144321. [[CrossRef](#)]
28. Zhang, L.; Li, W.; Li, J.; Xie, H.; Zhao, W. A novel iron-mediated nitrogen removal technology of ammonium oxidation coupled to nitrate/nitrite reduction: Recent advances. *J. Environ. Manag.* **2022**, *319*, 115779. [[CrossRef](#)] [[PubMed](#)]
29. Qiu, L. *Iron-Mediated Sulfur Autotrophic Denitrification System for Improving Deep Nitrogen Removal from Landfill Leachate*; Guangzhou University: Guangzhou, China, 2023.
30. Straub, K.L.; Benz, M.; Schink, B.; Widdel, F. Anaerobic, nitrate-dependent microbial oxidation of ferrous iron. *Appl. Environ. Microbiol.* **1996**, *62*, 1458–1460. [[CrossRef](#)] [[PubMed](#)]
31. Kelly, D.P.; Wood, A.P. *Halothiobacillus*; John Wiley & Sons, Ltd.: Hoboken, NJ, USA, 2015.
32. Vikromvarasiri, N.; Pisutpaisal, N. Hydrogen sulfide removal in biotrickling filter system by *Halothiobacillus neapolitanus*. *Int. J. Hydrog. Energy* **2016**, *41*, 15682–15687. [[CrossRef](#)]
33. Tan, X. *Study on the Diversity of Sulfur Oxidizing Bacteria and Their Thiometabolic Pathways in Pearl River Water*; South China University of Technology: Guangzhou, China, 2016.
34. Rickard, D.; Luther, G.W. Chemistry of Iron Sulfides. *Chem. Rev.* **2007**, *107*, 514–562. [[CrossRef](#)]
35. Han, S.; Cui, Y.; Yan, H.; Cui, Y.; Chen, Z. Enhancing simultaneous nitrate and phosphate removal in sulfur-iron (II) autotrophic denitrification biofilters by endogenous magnetic fields: Performance and mechanism. *J. Water Process Eng.* **2023**, *53*, 103767. [[CrossRef](#)]
36. Zhang, Y.; Wei, D.; Morrison, L.; Ge, Z.; Zhan, X.; Li, R. Nutrient removal through pyrrhotite autotrophic denitrification: Implications for eutrophication control. *Sci. Total Environ.* **2019**, *662*, 287–296. [[CrossRef](#)]
37. Xia, D.; Li, Y.; Huang, G.; Yin, R.; An, T.; Li, G.; Zhao, H.; Lu, A.; Wong, P.K. Activation of persulfates by natural magnetic pyrrhotite for water disinfection: Efficiency, mechanisms, and stability. *Water Res.* **2017**, *112*, 236–247. [[CrossRef](#)]
38. Hu, S.; Wu, G.; Li, R.; Xiao, L.; Zhan, X. Iron sulphides mediated autotrophic denitrification: An emerging bioprocess for nitrate pollution mitigation and sustainable wastewater treatment. *Water Res.* **2020**, *179*, 115914. [[CrossRef](#)] [[PubMed](#)]

39. Zhang, H.; Sun, M.; Tian, J.; Zhu, X.; Cheng, Y. Synergetic effects of pyrrhotite and biochar on simultaneous removal of nitrate and phosphate in autotrophic denitrification system. *Water Environ. Res.* **2023**, *95*, e10855. [[CrossRef](#)] [[PubMed](#)]
40. Chen, X.; Yang, L.; Chen, F.; Song, Q.; Feng, C.; Liu, X.; Li, M. High efficient bio-denitrification of nitrate contaminated water with low ammonium and sulfate production by a sulfur/pyrite-based bioreactor. *Bioresour. Technol.* **2022**, *346*, 126669. [[CrossRef](#)] [[PubMed](#)]

Disclaimer/Publisher's Note: The statements, opinions and data contained in all publications are solely those of the individual author(s) and contributor(s) and not of MDPI and/or the editor(s). MDPI and/or the editor(s) disclaim responsibility for any injury to people or property resulting from any ideas, methods, instructions or products referred to in the content.